

Investigating the signs of evolutionary characteristics in the energy spectrum of shock wave acceleration

Xu-Lin Dong

*College of Physics, Hebei Normal University, No. 20 Road East 2nd Ring South, Shijiazhuang, 050024 Hebei, China and
Key Laboratory of Particle Astrophysics, Institute of High Energy Physics,
Chinese Academy of Sciences, No. 19 B Yuquan Road, Shijingshan District, Beijing, 100049, China*

Wei-Kang Gao

*Key Laboratory of Particle Astrophysics, Institute of High Energy Physics,
Chinese Academy of Sciences, No. 19 B Yuquan Road,
Shijingshan District, Beijing, 100049, China and
University of Chinese Academy of Sciences, No. 19 A Yuquan Road, Shijingshan District Beijing 100049, China*

Yi-Qing Guo*

*Key Laboratory of Particle Astrophysics, Institute of High Energy Physics,
Chinese Academy of Sciences, No. 19 B Yuquan Road, Shijingshan District Beijing 100049, China
University of Chinese Academy of Sciences, No. 19 A Yuquan Road, Shijingshan District Beijing 100049, China and
TIANFU Cosmic Ray Research Center, No. 1500 Kezhi Road Chengdu, 610101 Sichuan, China*

Shu-Wang Cui†

*College of Physics, Hebei Normal University, No. 20 Road East 2nd Ring South, Shijiazhuang, 050024 Hebei, China and
TIANFU Cosmic Ray Research Center, No. 1500 Kezhi Road Chengdu, 610101 Sichuan, China*

Under ideal conditions, the theory of shock acceleration for cosmic rays predicts that different elements should exhibit strictly identical spectral indices (γ) when accelerated to the same rigidity (R). However, recent high-precision measurements of elemental energy spectra have definitively established the existence of variations in spectral indices (γ) across different elements. This study constrains the spectral indices (γ) of cosmic-ray elements using AMS-02 and DAMPE observations within the Spatially Dependent Propagation (SDP) model. For elements with $A/Z \approx 2$, γ shows significant positive correlations with both atomic number Z and mass number A , likely due to A or Z -dependent fragmentation cross-sections. Predictions indicate that the observed spectra of Ni and Zn will align with the Fe spectrum, while their injection spectra will exhibit slightly softer spectral indices compared to Fe. Future observations from AMS-02, DAMPE and HERD are expected to verify these findings, while theoretical models are needed to systematically explain this phenomenon.

I. INTRODUCTION

The acceleration mechanism is one of the three fundamental questions in cosmic-ray research, serving as a critical link between the origin and propagation of cosmic rays. It determines the maximum energy achievable by cosmic-ray sources and shapes the spectral form of their injection. Shock acceleration is widely accepted as the standard mechanism for cosmic-ray acceleration. Under ideal conditions, the spectral index γ of accelerated particles approximately follows: $\gamma = 3\sigma/(\sigma - 1)$ [1–3], where σ denotes the shock compression ratio. This implies that different elements should exhibit the same γ value at a given rigidity.

However, recent observations from the AMS-02 experiment[4–10] have revealed systematic differences in the energy spectra of various elements, with particularly notable discrepancies between groups of primary

elements—specifically the He-C-O-Fe group and the Ne-Mg-Si-S group[7]. Dong et al[11]. suggested that these differences might arise from a higher fraction of secondary contributions in the Ne-Mg-Si-S group. Nevertheless, their study still reported non-negligible variations in γ across elements. Similarly, Pan et al[12]., in their analysis of AMS-02 spectral data, also concluded that the values of γ differ among elements.

A clear tension exists between the theoretical expectation of a universal γ and the experimentally observed dependence on elemental species. Although the differences in γ could be attributed to variations in elemental origins[12], such an explanation appears contrived and lacks naturalness. Therefore, we aim to systematically investigate the physical principles underlying the divergence in γ , which may contribute to the advancement of acceleration theory.

In this work, employing a spatially-dependent propagation model (SDP model)[13–17] and using experimental data from AMS-02 and DAMPE[18], we constrain the values of γ and find that γ increases with atomic mass A or atomic number Z . We propose that this trend may be related to the larger fragmentation cross-sections of heav-

* guoyq@ihep.ac.cn

† cuisw@hebtu.edu.cn

TABLE I: Propagation model parameters.

D_0 [cm ⁻² s ⁻¹]	δ_0	N_m	ξ	n	v_A [km s ⁻¹]	z_0 [kpc]
5.7×10^{28}	0.58 ^a	0.24	0.082	4.0	6	5

^a When fitting the DAMPE data $\delta_0 = 0.65$.

TABLE II: Spectral injection parameters.

Element	Normalization		Abundance
	[GeV ⁻¹ m ⁻² s ⁻¹ sr ⁻¹]	γ_2 ^a	
He	2.54×10^{-3}	$2.34^{+0.01b}_{-0.01}$	74550
C	9.41×10^{-5}	$2.36^{+0.01c}_{-0.01}$	2760
N	5.63×10^{-6}	$2.34^{+0.01}_{-0.01}$	165
O	1.23×10^{-4}	$2.37^{+0.02d}_{-0.02}$	3600
Ne	1.79×10^{-5}	$2.38^{+0.02}_{-0.02}$	526
Na	5.45×10^{-7}	$2.40^{+0.01}_{-0.01}$	16
Mg	2.33×10^{-5}	$2.40^{+0.02}_{-0.02}$	684
Al	1.67×10^{-6}	$2.39^{+0.01}_{-0.01}$	49
Si	2.36×10^{-5}	$2.40^{+0.02}_{-0.02}$	691
S	3.89×10^{-6}	$2.41^{+0.02}_{-0.02}$	114
Fe	2.50×10^{-5}	$2.42^{+0.03e}_{-0.02}$	734

^a γ_2 is constrained by $\chi^2/\text{d.o.f.} < 2$, $\gamma_1 = 2.10$, $R_{br} = 8\text{GV}$.

^b When fitting the DAMPE data $\gamma_2 = 2.32^{+0.01}_{-0.01}$.

^c When fitting the DAMPE data $\gamma_2 = 2.33^{+0.01}_{-0.01}$.

^d When fitting the DAMPE data $\gamma_2 = 2.35^{+0.01}_{-0.01}$.

^e When fitting the DAMPE data $\gamma_2 = 2.40^{+0.01}_{-0.02}$.

ier nuclei, which undergo more significant fragmentation during acceleration, leading to a predictable modification of the spectral index.

II. MODEL AND METHODOLOGY

In the following, a quantitative description of the CR propagation process is provided. The propagation of CRs can be represented mathematically by the following partial differential equation[19]

$$\frac{\partial \Psi(\vec{r}, p, t)}{\partial t} = Q(\vec{r}, p, t) + \vec{\nabla} \cdot (D_{xx} \vec{\nabla} \Psi - \vec{V}_c \Psi) + \frac{\partial}{\partial p} [p^2 D_{pp} \frac{\partial \Psi}{\partial p} p^2] - \frac{\partial}{\partial p} [\dot{p} \Psi - \frac{p}{3} (\vec{\nabla} \cdot \vec{V}_c)] - \frac{\psi}{\tau_f} - \frac{\psi}{\tau_r}, \quad (1)$$

where $Q(\vec{r}, p, t)$ describes the distribution of sources, \vec{V}_c represents the convection velocity, D_{pp} is the momentum diffusion coefficient accounting for the reacceleration process, \dot{p} , τ_f and τ_r are the energy loss rate, the fragmentation timescale, and the radioactive decay timescale, respectively.

The SDP model divides the cosmic ray diffusion region into two parts: the inner zone is a cylindrical area centered on the galactic disk plane and extending a certain thickness on both sides, while the remaining areas constitute the outer zone. The diffusion speed of CRs in the inner zone is lower than that in the outer zone and

depends on the distribution of sources. The diffusion coefficient of the model is expressed as:

$$D_{xx}(r, z, R) = D_0 F(r, z) \beta^n \left(\frac{R}{R_0} \right)^{\delta(r, z)}, \quad (2)$$

where the function $F(r, z)$ is defined as:

$$F(r, z) = \begin{cases} g(r, z) + [1 - g(r, z)] \left(\frac{z}{\xi z_0} \right)^n, & |z| \leq \xi z_0 \\ 1, & |z| > \xi z_0 \end{cases}, \quad (3)$$

With $g(r, z) = N_m / [1 + f(r, z)]$. Here the diffusion coefficient of the inner zone is anticorrelated with the source distribution $f(r, z)$, given by

$$f(r, z) = \left(\frac{r}{r_\odot} \right)^{1.25} \exp \left[-\frac{3.87(r - r_\odot)}{r_\odot} \right] \exp \left(-\frac{|z|}{z_s} \right), \quad (4)$$

where $r_\odot = 8.5$ kpc and $z_s = 0.2$ kpc. For the outer zone, the diffusion coefficient remains constant when varying spatial locations. In contrast, the diffusion coefficient in the traditional model remains constant throughout the entire space.

The source spectrum of CRs is assumed to be a broken power law in rigidity.

$$q(R) \propto \begin{cases} \left(\frac{R}{R_{br}} \right)^{-\gamma_1}, & R < R_{br} \\ \left(\frac{R}{R_{br}} \right)^{-\gamma_2}, & R \geq R_{br} \end{cases} \quad (5)$$

To solve the transport equation, we employ the numerical package DRAGON[20]. The force field approximation is incorporated to account for solar modulation effects[21]. The key parameters related to the SDP model are summarized in Table I, while the spectral parameters of each element are summarized in Table II. Since there are slight differences in the spectral indices measured by the AMS-02 and DAMPE experiments, we performed separate fits to the data from both experiments, adjusted some parameters accordingly, and marked the corresponding entries in the tables.

III. RESULTS

Based on the above configuration, our calculations successfully reproduce the energy spectral fluxes of He, C, O, Ne, Mg, Si, S, Fe, N, Na, and Al as measured by AMS-02, as well as those of He, C, O, and Fe obtained by DAMPE. To minimize potential influences from solar modulation effects, we focus our analysis on the relationship between γ_2 and the atomic mass number A as well as the atomic number Z. The specific results are shown in Figure 1.

The top-left panel of Figure 1 displays the relationship between γ_2 and A derived from the AMS-02 data, with a

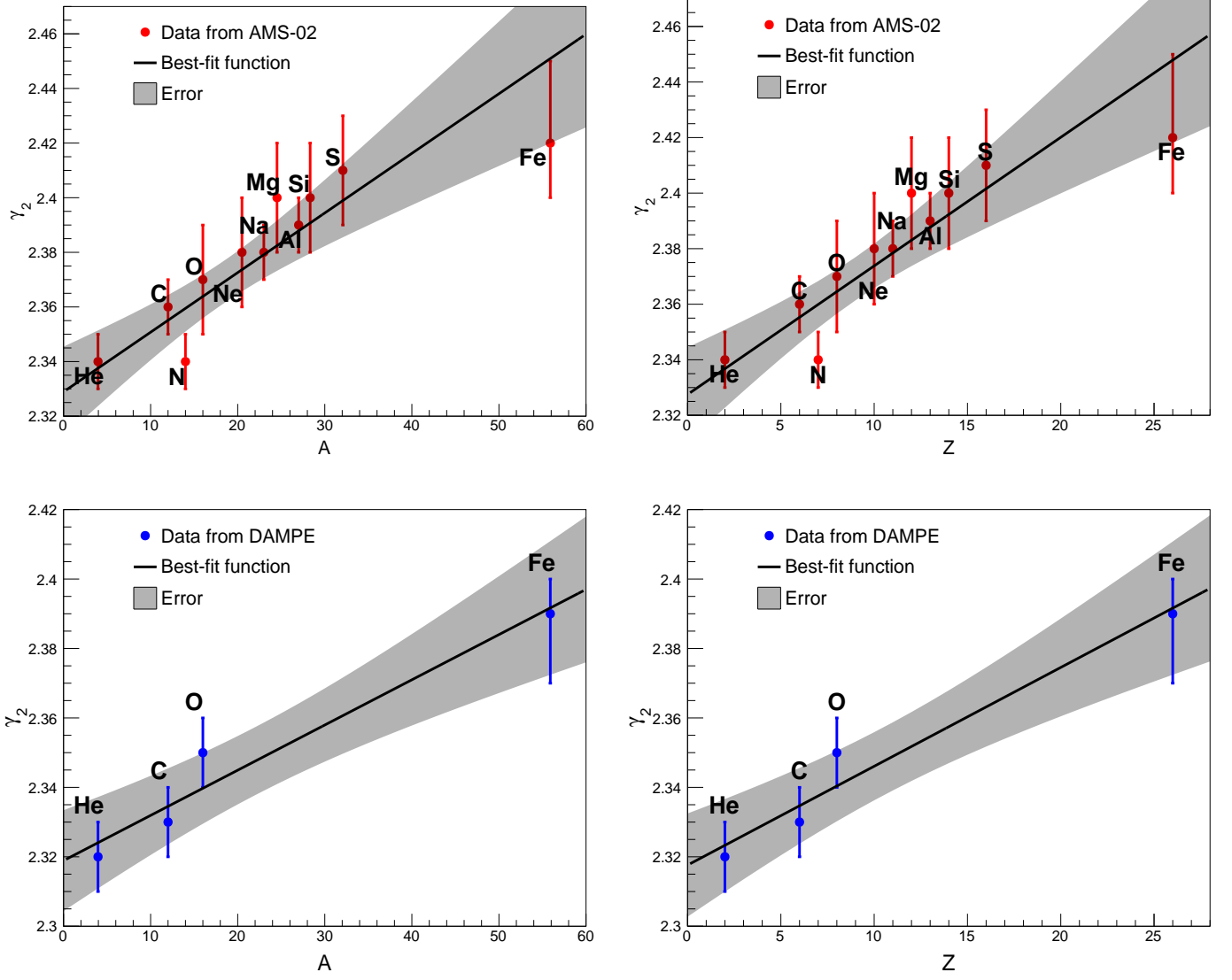


FIG. 1: Correlation between the injection spectral index γ_2 and the nucleon number A or proton number Z for various elements. The red and blue data points represent the fitting results derived from the AMS-02 and DAMPE data, respectively. The uncertainties in γ_2 were determined by constraining $\chi^2/\text{d.o.f.} < 2$. The solid red and blue lines correspond to the linear fits to the AMS-02 and DAMPE data, respectively, with the shaded areas indicating the associated uncertainties of the fits. Top left: γ_2 as a function of A from AMS-02; Top right: γ_2 as a function of Z from AMS-02; Bottom left: γ_2 as a function of A from DAMPE; Bottom right: γ_2 as a function of Z from DAMPE.

correlation coefficient of $r = 0.73^{+0.17}_{-0.17}$ ($p = 0.005$). The linear fit yields:

$$\gamma_2 = 0.0022^{+0.0004}_{-0.0004}A + 2.329^{+0.008}_{-0.008} \quad (6)$$

, with $\chi^2/\text{d.o.f.} = 6.70/9$. The top-right panel shows the relationship between γ_2 and Z based on the AMS-02 data, also exhibiting a correlation coefficient of $r = 0.73^{+0.17}_{-0.17}$ ($p = 0.0043$). The linear regression result is:

$$\gamma_2 = 0.0046^{+0.0009}_{-0.0009}Z + 2.328^{+0.009}_{-0.009} \quad (7)$$

, with $\chi^2/\text{d.o.f.} = 6.45/9$. The bottom-left panel presents the relationship between γ_2 and A from the DAMPE

dataset, which similarly gives a correlation coefficient of $r = 0.72^{+0.18}_{-0.18}$ ($p = 0.582$). The linear fit result is:

$$\gamma_2 = 0.0013^{+0.0002}_{-0.0002}A - 2.319^{+0.007}_{-0.007} \quad (8)$$

, with $\chi^2/\text{d.o.f.} = 1.45/2$. The bottom-right panel illustrates the relationship between γ_2 and Z based on the DAMPE data, with a correlation coefficient of $r = 0.72^{+0.18}_{-0.18}$ ($p = 0.575$). The linear regression gives:

$$\gamma_2 = 0.0028^{+0.0005}_{-0.0005}Z + 2.318^{+0.008}_{-0.008} \quad (9)$$

, with $\chi^2/\text{d.o.f.} = 1.28/2$.

Taken together, these results clearly indicate a significant positive correlation between γ_2 and both A and

Z for elements with $A/Z \approx 2$. We speculate that this phenomenon may be related to the fragmentation effect during the acceleration process: nuclei with larger mass numbers A possess larger fragmentation cross-sections, leading to greater losses due to fragmentation during acceleration, which ultimately softens the energy spectrum. Alternatively, this result could also stem from differences in energy loss during the injection and acceleration processes among different elements.

IV. DISCUSSION

The results of this study cannot yet account for the softer proton injection spectrum. This phenomenon is generally attributed to the injection rate of particles into the acceleration region[22]. Based on the results presented here, we anticipate $\gamma_{\text{Ni}} \approx \gamma_{\text{Zn}} \approx 2.44$ [23]. Given that Ni and Zn contain no secondary components, their energy spectra are expected to be similar to that of iron. The currently limited number of elemental energy spectra measured by DAMPE leads to an elevated p-value. Therefore, we anticipate that future observations from AMS-02, DAMPE, and HERD will provide more data to further verify and confirm this result.

V. CONCLUSIONS

Based on observational data from AMS-02 and DAMPE, this study confirms a positive correlation be-

tween the injection spectral index γ of various elements in cosmic rays and both the nucleon number A and the proton number Z. We hypothesize that this relationship may be associated with collisional fragmentation effects experienced by elements during the acceleration process.

ACKNOWLEDGMENTS

We gratefully acknowledge Lin Nie, Zigui Dong, and others for their substantial assistance and valuable suggestions in the completion of this work. This work was financially supported by the National Key R&D Program of China (Grant No. 2025SKA0110103), the National Natural Science Foundation of China (Grants No. 12333006, 12275279, 12373105, and 12320101005), and the Postgraduate Innovation Fund Project of Hebei Provincial Education Department (Grant No. CXZZBS2026083).

Appendix A: The Injection Spectra and Energy Spectra in the SDP Model

-
- [1] E. G. Berezhko and G. F. Krymskiĭ, Reviews of topical problems: Acceleration of cosmic rays by shock waves, *Soviet Physics Uspekhi* **31** (1988).
 - [2] L. O. Drury, An introduction to the theory of diffusive shock acceleration of energetic particles in tenuous plasmas, *Reports on Progress in Physics* **46**, 973 (1983).
 - [3] L. I. Dorman, *Cosmic ray interactions, propagation, and acceleration in space plasmas* (Springer, 2006).
 - [4] M. Aguilar, L. A. Cavasonza, G. Ambrosi, L. Arruda, N. Attig, F. Barao, L. Barrin, A. Bartoloni, S. Başğmezdu Pree, J. Bates, *et al.*, The alpha magnetic spectrometer (ams) on the international space station: Part ii—results from the first seven years, *Physics reports* **894**, 1 (2021).
 - [5] M. Aguilar, B. Alpat, G. Ambrosi, H. Anderson, L. Arruda, N. Attig, C. Bagwell, F. Barao, M. Barbanera, L. Barrin, *et al.*, Properties of cosmic deuterons measured by the alpha magnetic spectrometer, *Physical review letters* **132**, 261001 (2024).
 - [6] M. Aguilar, L. Ali Cavasonza, B. Alpat, G. Ambrosi, L. Arruda, N. Attig, C. Bagwell, F. Barao, L. Barrin, A. Bartoloni, *et al.*, Properties of cosmic-ray sulfur and determination of the composition of primary cosmic-ray carbon, neon, magnesium, and sulfur: Ten-year results from the alpha magnetic spectrometer, *Physical review letters* **130**, 211002 (2023).
 - [7] M. Aguilar, L. A. Cavasonza, B. Alpat, G. Ambrosi, L. Arruda, N. Attig, F. Barao, L. Barrin, A. Bartoloni, S. Başğmezdu Pree, *et al.*, Properties of a new group of cosmic nuclei: results from the alpha magnetic spectrometer on sodium, aluminum, and nitrogen, *Physical review letters* **127**, 021101 (2021).
 - [8] M. Aguilar, L. A. Cavasonza, M. Allen, B. Alpat, G. Ambrosi, L. Arruda, N. Attig, F. Barao, L. Barrin, A. Bartoloni, *et al.*, Properties of iron primary cosmic rays: Results from the alpha magnetic spectrometer, *Physical review letters* **126**, 041104 (2021).
 - [9] M. Aguilar, L. Ali Cavasonza, G. Ambrosi, L. Arruda, N. Attig, F. Barao, L. Barrin, A. Bartoloni, S. Başğmezdu Pree, R. Battiston, *et al.*, Properties of neon, magnesium, and silicon primary cosmic rays results from the alpha magnetic spectrometer, *Physical review letters* **124**, 211102 (2020).
 - [10] M. Aguilar, L. Ali Cavasonza, G. Ambrosi, L. Arruda, N. Attig, A. Bachlechner, F. Barao, A. Barrau, L. Barrin, A. Bartoloni, *et al.*, Properties of cosmic helium isotopes measured by the alpha magnetic spectrometer, *Physical review letters* **123**, 181102 (2019).
 - [11] X.-L. Dong, Y.-H. Yao, Y.-Q. Guo, and S.-W. Cui, New understanding of nuclei spectra properties observed by

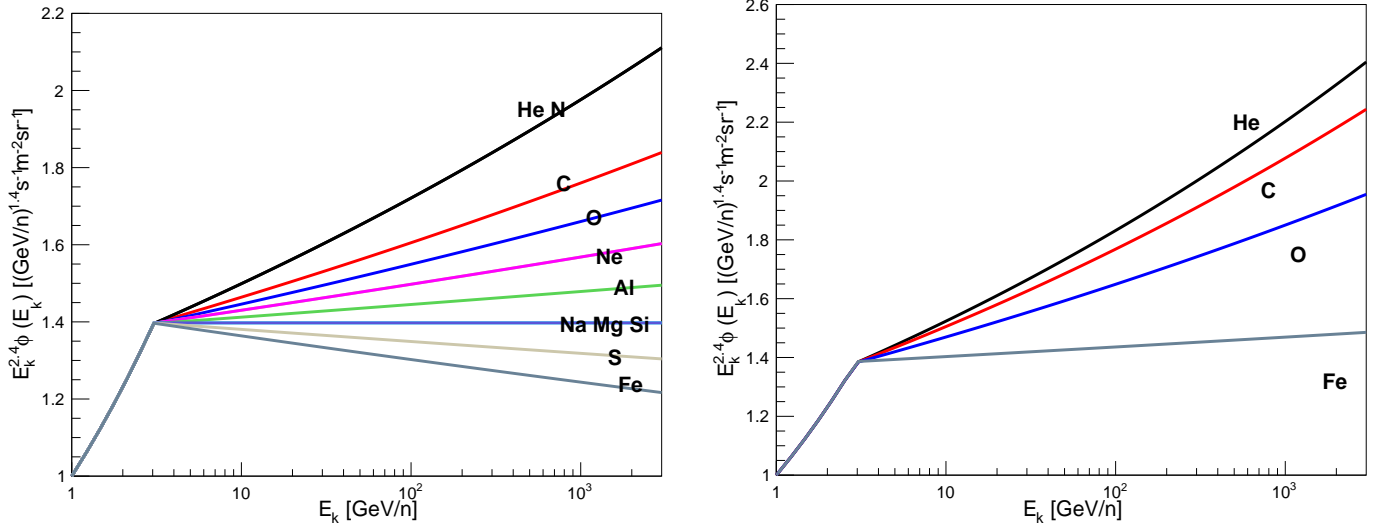


FIG. 2: The injection energy spectra of various elements derived from the spatially dependent propagation (SDP) model fitting to AMS-02 data (left) and DAMPE data (right).

the ams-02 experiment, *Physical Review D* **109**, 063027 (2024).

- [12] X. Pan and Q. Yuan, Injection spectra of different species of cosmic rays from ams-02, ace-cris and voyager-1, *Research in Astronomy and Astrophysics* **23**, 115002 (2023).
- [13] N. Tomassetti, Origin of the cosmic-ray spectral hardening, *The Astrophysical Journal Letters* **752**, L13 (2012).
- [14] D. Gaggero, A. Urbano, M. Valli, and P. Ullio, Gamma-ray sky points to radial gradients in cosmic-ray transport, *Physical Review D* **91**, 083012 (2015).
- [15] Y.-Q. Guo, Z. Tian, and C. Jin, Spatial-dependent diffusion of cosmic rays and the ratio of pbar/p, b/c, arXiv preprint arXiv:1509.08227 (2015).
- [16] W. Liu, Y.-h. Yao, and Y.-Q. Guo, Revisiting the spatially dependent propagation model with the latest observations of cosmic-ray nuclei, *The Astrophysical Journal* **869**, 176 (2018).
- [17] A. Abeysekara, A. Albert, R. Alfaro, C. Alvarez, J. Álvarez, R. Arceo, J. Arteaga-Velázquez, D. Avila Rojas, H. Ayala Solares, A. Barber, *et al.*, Extended gamma-ray sources around pulsars constrain the origin of the positron flux at earth, *Science* **358**, 911 (2017).
- [18] F. Alemanno, Q. An, P. Azzarello, F.-C.-T. Barbato, P. Bernardini, X.-J. Bi, H. V. Boutin, I. Cagnoli, M.-S. Cai, E. Casilli, *et al.*, Charge-dependent spectral softening of primary cosmic-rays from proton to iron below the knee, arXiv preprint arXiv:2511.05409 (2025).
- [19] D. Maurin, R. Taillet, F. Donato, P. Salati, A. Barrau, and G. Boudoul, Galactic cosmic ray nuclei as a tool for astroparticle physics, arXiv preprint astro-ph/0212111 (2002).
- [20] C. Evoli, D. Gaggero, D. Grasso, and L. Maccione, Cosmic ray nuclei, antiprotons and gamma rays in the galaxy: a new diffusion model, *Journal of Cosmology and Astroparticle Physics* **2008** (10), 018.
- [21] L. Gleeson and W. Axford, Solar modulation of galactic cosmic rays, *Astrophysical Journal*, vol. 154, p. 1011 **154**, 1011 (1968).
- [22] A. Hanusch, T. Liseykina, and M. Malkov, Anomalies in cosmic ray composition: Explanation based on mass to charge ratio, arXiv preprint arXiv:1707.02744 (2017).
- [23] O. Adriani, Y. Akaike, K. Asano, Y. Asaoka, E. Berti, G. Bigongiari, W. Binns, M. Bonghi, P. Brogi, A. Bruno, *et al.*, Direct measurements of cosmic-ray iron and nickel with calet on the international space station, *Advances in Space Research* **74**, 4368 (2024).

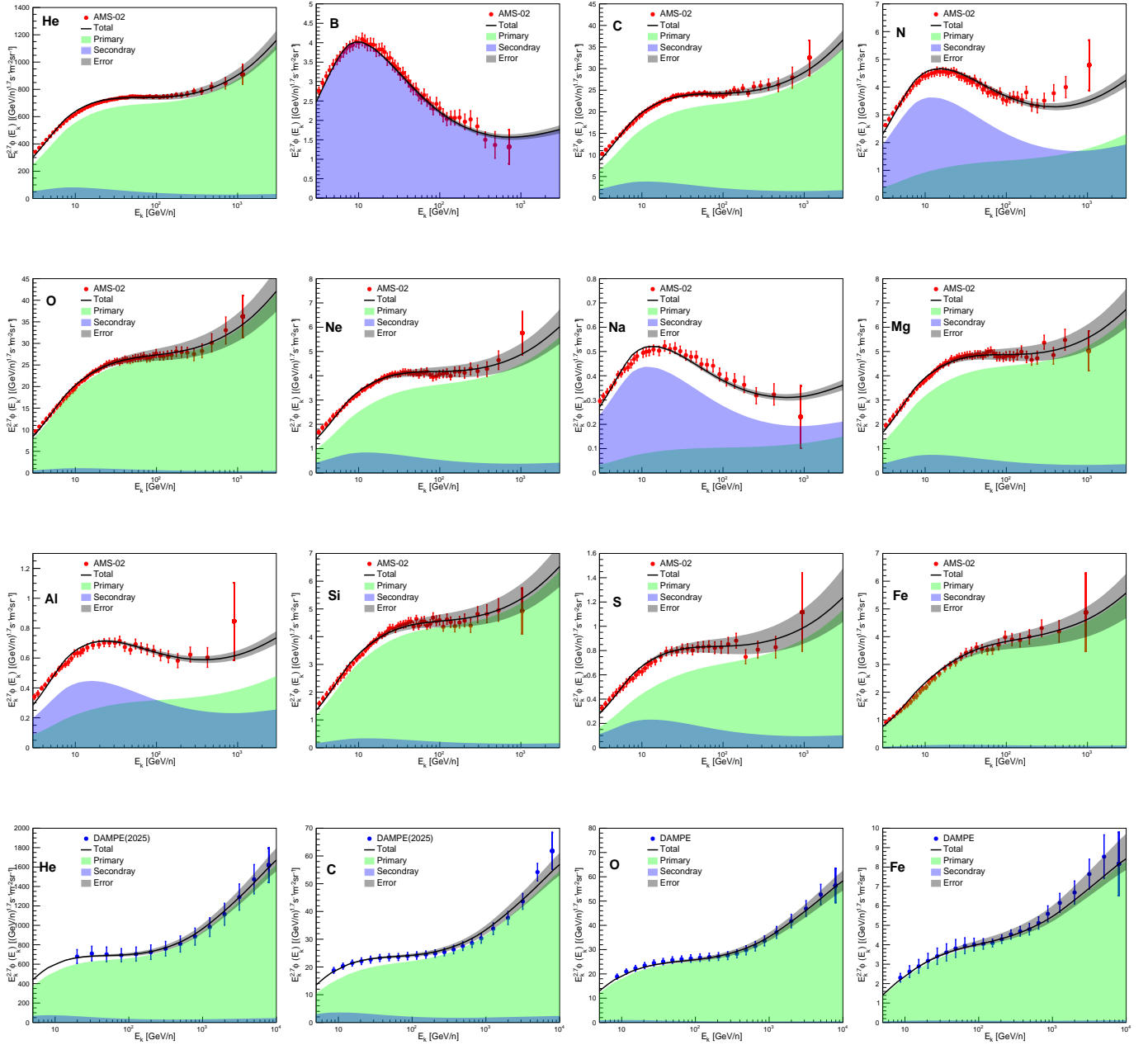


FIG. 3: The fluxes of various elements calculated by the model are compared with the experimental observations from AMS-02 and DAMPE. In the figure, red points represent AMS-02 observational results, blue points represent DAMPE observational results, the black solid line denotes the total flux calculated by the model, and the shaded black area indicates the error range obtained under the condition of $\chi^2/\text{d.o.f.} < 2$. "Primary" and "Secondary" refer to the energy spectra of the primary and secondary components, respectively.